Crystal Structure Refinement of Synthetic Pure Gyrolite

Arūnas BALTUŠNIKAS [1, 2] *, **Raimundas ŠIAUČIŪNAS [2]**, **Irena LUKOŠIŪTĖ [1]**, **Kęstutis BALTAKYS [2]**, **Anatolijus EISINAS [2]**, **Rita KRIŪKIENĖ [1]**

[1] *Lithuanian Energy Institute, Breslaujos 3, LT-44403 Kaunas, Lithuania*
[2] *Department of Silicate Technology, Kaunas University of Technology, Radvilenu 19, LT-50254 Kaunas, Lithuania*

Pure calcium silicate hydrate – gyrolite was prepared under the saturated steam pressure at 473 K temperature in rotating autoclave. The crystal structure of synthetic gyrolite was investigated by X-ray diffraction and refined using Le Bail, Rietveld and crystal structure modelling methods. Background, peak shape parameters and verification of the space group $P\bar{1}$ were performed by the Le Bail full pattern decomposition. Peculiarities of interlayer sheet *X* of gyrolite unit cell were highlighted by Rietveld refinement. Possible atomic arrangement in interlayer sheet *X* was solved by global optimization method. Most likelihood crystal structure model of gyrolite was calculated by final Rietveld refinement. It was crystallographically showed, that cell parameters are: $a = 0.9713(2)$ nm, $b = 0.9715(2)$ nm, $c = 2.2442(3)$ nm and $\alpha = 95.48(2)°$, $\beta = 91.45(2)°$, $\gamma = l20.05(3)°$.

Keywords: gyrolite, crystal structure, XRD, Le Bail fitting, Rietveld refinement, global optimization.

1. INTRODUCTION

Recently, the interest of gyrolite group compounds (gyrolite, Z-phase, truscottite, reyerite) increases because the new possibilities of application were found: it may be used to reduce heavy metal ions and remove them from wastewaters [1–5]. It was shown that gyrolite sorption properties are greater than tobermorite group minerals [6–8]. Of specific interest is the purported ability of gyrolite to separate super coiled plasmid, open circular plasmid, and genomic DNA [9]. Moreover, the ion-exchange properties of gyrolite were applied for creation new organically modified filler for polymeric nanocomposites [10].

Gyrolite $(Ca_{16}Si_{24}O_{60}(OH)_8 \cdot (14+x)H_2O$ usually occurs as a natural mineral in association with zeolites and often forms nodular aggregates. These aggregates can appear glassy, dull or even fibrous. Gyrolite can be synthesized from CaO and various forms of SiO_2 with the molar ratio CaO/SiO_2 (C/S=0.66) in aqueous suspension at temperatures of about 473 K. Physical, chemical properties and some aspects of structure of gyrolite were studied by many scientists [11–16]. However, their opinions differ. One of the reasons that the properties of gyrolite have not been analyzed in detail is that the synthesis of this compound is complex, and it is still rarely applied in practice.

Some properties (like sorption capacity) depend not only on the crystal lattice of a porous body but also on that of the surface microstructure and specific surface area, as well as on the dominant pore size and their differential distribution in the material according to the radius. In the case of gyrolite crystal lattice, these properties usually depend on the proportion of crystalline and in some level disordered crystal lattice structural parts. However, no data were found in references about the influence of synthesis conditions on gyrolite crystal lattice.

Attempts to solve the crystal chemistry of mineral gyrolite was carried out by many researchers but the last and most comprehensive determination of a crystal structure and unit cell parameters of a natural mineral gyrolite was performed by Merlino S. [17]. He established that gyrolite has triclinic symmetry and the space group $P\bar{1}$. The unit cell dimensions were found to be $a = 9.74(1)$ Å, $b = 9.74(1)$ Å, $c = 22.40(1)$ Å, $\alpha = 95.7(1)°$, $\beta = 91.5(1)°$, $\gamma = l20.0(1)°$ and the crystal chemical formula which accounts for most gyrolite samples is $Ca_{16}Si_{24}O_{60}(OH)_8 \cdot (14+x)H_2O$, with $0 \le x \le 3$. Reviewing previous investigations Merlino S. summarized that gyrolite is closely structurally related with minerals – truscottite $Ca_{14}Si_{24}O_{58}(OH)_8 \cdot 2H_2O$ symmetry $P\bar{3}$, unit cell parameters $a = 9.731(2)$ Å, $c = 18.84(1)$ Å, $\alpha = 90°$, $\beta = 90°$, $\gamma = 120°$ [18] and reyerite (Na, K)$_2Ca_{14}Si_{22}Al_2O_{58} \cdot 6H_2O$ space group $P\bar{3}$, unit cell parameters $a = 9.765(3)$ Å, $c = 19.067(3)$ Å, $\alpha = 90°$, $\beta = 90°$, $\gamma = 120°$ [19]. The above mentioned minerals crystal structure is built up by the stacking of various structural layers, which are made up of octahedral calcium sheets *O* and single and double sheets of silicon and aluminum tetrahedra, S_1 and $S_2\overline{S_2}$ respectively (Fig. 1) [17]. The only substantial structural difference among these minerals is the presence of three (Ca, Na)-octahedra in the interlayer sheet *X* of gyrolite between the tetrahedral sheets S_2 and $\overline{S_2}$ which, in the reyerite and truscotite, are directly connected to form a double layer [17–20]. Moreover, Ferraris G. *at al*. also showed a close structural relationship between tungusite and gyrolite. In tungusite interlayer sheet *X*, which in gyrolite contains only 3(Ca, Na), can be filled up to nine cations and the following ideal formula of the unit cell was obtained for tungusite: $[Ca_{14}(OH)_8](Si_8O_{20})(Si_8O_{20})_2[M_9^{2+}(OH)_{14}]$ symmetry $P\bar{1}$ and unit cell parameters $a = 9.714(9)$ Å, $b = 9.721(9)$ Å, $c = 22.09(3)$ Å, $\alpha = 90.13(1)°$, $\beta = 98.3(2)°$, $\gamma = 120.0(1)°$ [20].

---

*Corresponding author. Tel.: +370-37-401906, fax: +370-37-351271.
E-mail address: *abalt@mail.lei.lt* (A. Baltušnikas)

The structures of earlier mentioned natural minerals have been solved with conventional single-crystal X-ray structural analysis. On the other hand, it is very important to be able to perform structural analysis of synthetic layered silicates using conventional powder X-ray diffraction and Rietveld techniques. It should be noted that such kind of analysis in this area are rare. Renaudin G. et al. [21] performed Rietveld refinement of C-S-H and C-A-S-H phase's crystal structure of similar compositions to gyrolite. They have refined all (over 40) describing the structure and microstructure parameters. Stumm A., Garbev K. et al. [22] using Rietveld analysis have investigated the incorporation of zinc into the interlayer sheet *X* of calcium silicate hydrate – gyrolite. No more data were found in literature about the crystal structure refinement of synthetic gyrolite using Rietveld refinement.

Based on literature review it can be considered that the most probable changes of crystal structure parameters during synthesis, modification or processing of gyrolite could occur mainly in the interlayer sheet *X*. Previously, using theoretical model of gyrolite crystal structure, it was shown that the Rietveld method is suitable not only for the crystal lattice parameters refinement but also for refinement of all atomic coordinates and the fractional occupancy of cations, intercalated in the interlayer sheet of crystal lattice. As well, it was proved that the refinement of all gyrolite crystal structure parameters could be achieved only using restraints on bond lengths [23].

In this article the Rietveld refinement method has been applied for purpose to determine the peculiarities of structural parameters of pure gyrolite synthesized in laboratory at hydrothermal conditions.

2. EXPERIMENTAL

Pure calcium silicate hydrate – gyrolite used in this study was synthesized in Kaunas University of Technology Department of Silicate Technology. Hydrothermal synthesis of gyrolite has been carried out in rotating autoclave Parr Instrument (10 rpm) under the saturated steam pressure at 473 K; the duration of isothermal curing was 72 hours. The molar ratio of primary mixture was $CaO/SiO_2 = 0.66$. These synthesis conditions were chosen according to the previously published data [16]. The experimental X-ray diffraction pattern of synthetic gyrolite was recorded from a front-packed flat plate specimen on a DRON-6 diffractometer. X-ray tube was set at 35 kV and 20 mA. The diffracted beam graphite monochromator was used for selection of CuK_α characteristic emission. Scanning was carried out at a step size of $0.02°$ (2θ) and counting time was 10 sec/step.

The X-ray diffraction profile of CeO_2 standard calcinated at 1573 K temperature for 5 hours was used for purpose to obtain the instrumental profile parameters of diffractometer used. To achieve this task peak shape and microstructural parameters were refined by the Le Bail's full pattern decomposition [24] using the GSAS+EXPGUI program package [25, 26]. The obtained instrumental profile parameters were used as starting values of profile parameters in the crystal structure refinement of synthetic pure gyrolite. The final refinement of crystal structure of synthetic pure gyrolite was performed by the Le Bail and

Rietveld structural refinement techniques using the GSAS+EXPGUI program too. All polyhedral crystal structure drawings were prepared by program DRAWxtl V5.3 [27]. The crystal structure data of natural gyrolite determined by Merlino S. have been employed as the initial structural model in the Rietveld refinement (Fig. 1).
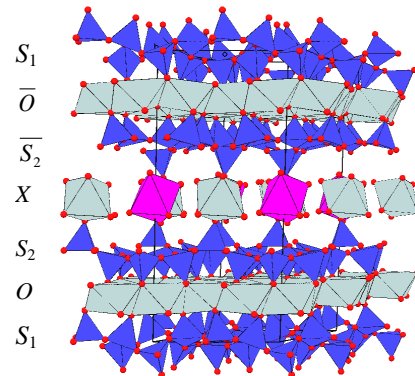

Fig. 1. Schematic drawing of a crystal structure of natural gyrolite with intercalated Na atoms as viewed perpendicular to axis *c*. Na-O octahedron depicted in pink

The structural parameters of gyrolite interlayer sheet *X* are presented in Table 1, wherein it is shown that the special position $(0, 0, 0.5)$ of gyrolite the unit cell is occupied by Ca or Na cations.

Table 1. Atomic positions, occupation parameters and isotropic temperature displacement parameters (U_{iso}) of the interlayer sheet *X* of natural mineral gyrolite [17]

Atom	x	y	z	Occupancy	U_{iso}, Å^2
Ca4	0.3302	0.6718	0.4983	1	0.05193
O1	0.2919	0.8740	0.5464	1	0.11019
O2	0.0784	0.5475	0.4391	1	0.10132
O3	0.3931	0.4892	0.4478	1	0.15198
O4	0.5877	0.8303	0.5582	1	0.15958
O5	0.7684	0.7748	0.4422	1	0.18998
O6	0.9470	0.8255	0.5864	1	0.20644
O7	0.8687	0.1174	0.5489	1	0.19758
Ca5(Na5)	0	0	0.5	1	0.17351

Merlino S. has found that in natural gyrolite this special position is occupied by Na cation (Fig. 1), however, in herein work, a Ca cation was located in this site during the initial refinement of crystal structure of synthetic pure gyrolite, because sodium atoms are absent (Fig. 2).
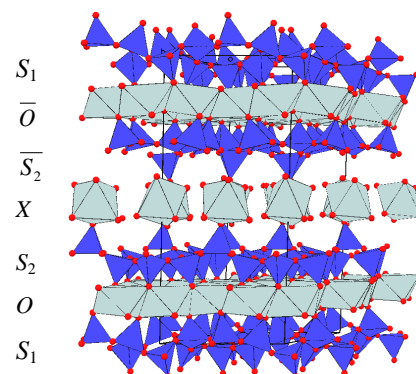

Fig. 2. Schematic drawing of a crystal structure of pure gyrolite as viewed perpendicular to axis *c*

In the final Rietveld refinement stage of crystal structure of pure synthetic gyrolite the program FOX and global optimization algorithm were applied for purpose to solve possible chemical composition and arrangement of atoms in the interlayer sheet *X* [28].

3. RESULTS AND DISCUSSION

Prior to the refinement of crystal structure the phase identification of as-synthesized gyrolite has been performed using PDF-2 Date base [29]. The analysis results are shown in Figure 3. It is evident that the all Bragg reflections are well matched by the patterns PDF no 42-1452 and PDF no 80-405 of gyrolite standards.
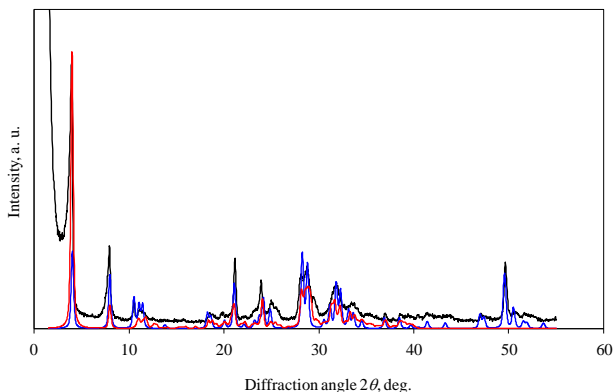

Fig. 3. The X-ray diffraction patterns of: synthetic pure gyrolite (in black), gyrolite standard PDF no 42-1452 (in blue), gyrolite standard PDF no 80-407 (in red)

The refinement of crystal structure of synthetic pure gyrolite was started from the background and the peak shape parameters refinement using the Le Bail full pattern decomposition. As well the verification of the space group $P\bar{1}$ for the synthetic pure gyrolite crystal structure was accomplished at this refinement stage. The resultant fitting plot is shown in Figure 4 in a standard Rietveld format. The fixed background points were manually selected and fitted by a combination of 36-parameters shifted-Chebyshev polynomial function via the EXPGUI menu using BKGEDIT program in GSAS.

Because some diffraction peaks are found at low Bragg angles of the X-ray pattern of gyrolite, the profile of the diffraction peaks was modelled using the third CW profile function (Pseudo-Voigt with Finger-Cox-Jephcoat peak asymmetry function) implemented in GSAS program [25]. The initial refinement of these 38 variables using 2675 observations yielded the weighted profile residual $R_{wp} = 5.18$ % and profile residual $R_p = 3.86$ % (Fig. 4).

Generally, during the final Rietveld refinement the background refinement optimization would be very useful. So, the simpler shape of the background would be more preferable than just refined one. For this purpose, in addition, the background subtraction was performed and linear one was obtained using the Le Bail full pattern decomposition as well the peak shape parameters refinement was continued (Fig. 5).The Le Bail refinement of following variables – linear background, peak shape and lattice parameters results in the reduction of weighted profile residual to $R_{wp} = 3.83$ % and profile residual to $R_p = 2.72$ %.
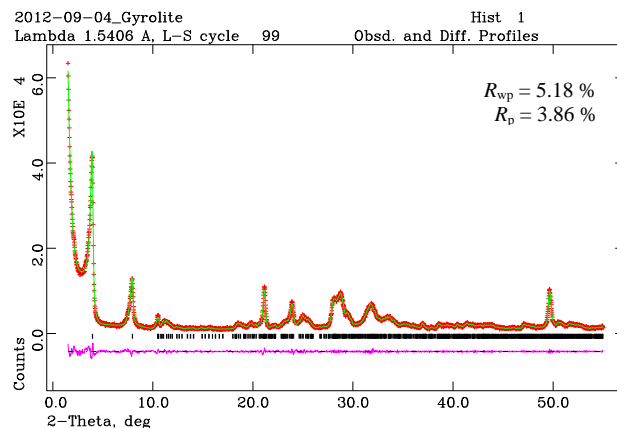

Fig. 4. The observed (in red), calculated (in green) and difference (in pink) X-ray diffraction patterns of synthetic pure gyrolite after Le Bail fitting. Calculated Bragg reflection positions are indicated by black lines for the gyrolite phase
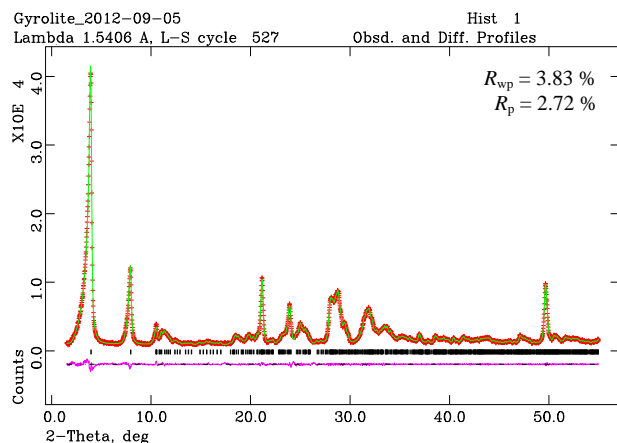

Fig. 5. The final Le Bail fitting plot of the observed (in red), refined (in green) and difference (in pink) between the observed and calculated patterns of pure gyrolite after the background subtraction

The Rietveld refinement of pure gyrolite crystal structure was started from the powder X-ray diffraction pattern calculation using the initial structural, microstructural and peak profile shape parameters determined during the initial Le Bail's fitting (Fig. 6).

Structural parameters haven't been refined at this stage and only scale factor was determined. The initial model of the crystal structure results in poor residuals: the weighted profile residual is $R_{wp} = 25.4$ % and profile residual is $R_p = 20.3$ % (Fig. 6).

For purpose to ensure the adequacy of the model the unit cell parameters, all atomic coordinates, all atomic displacement and atomic occupancy parameters of interlayer sheet *X* were refined in the next stage (Fig. 7). As have been established in our previous work [23] the refinement of gyrolite crystal structure should be performed using restraints (soft constraints) on bond lengths of Si-O = 0.162 nm and O-O = 0.263 nm in the tetrahedral sheets as well Ca-O = 0.24 nm, O-O = 0.34 nm and O-O = 0.48 nm – in the octahedral and in the interlayer sheets.

As we can see in Figure 7 the fit at this point of the Rietveld refinement is quite good. The resultant quality of the refinement is quantified by the corresponding figures

of merit: $R_{wp} = 11.9$ % and $R_p = 9.13$ % for a total of 196 refined parameters. The refined values of atomic coordinates and fractional occupancy of the interlayer sheet X are shown in Table 2.
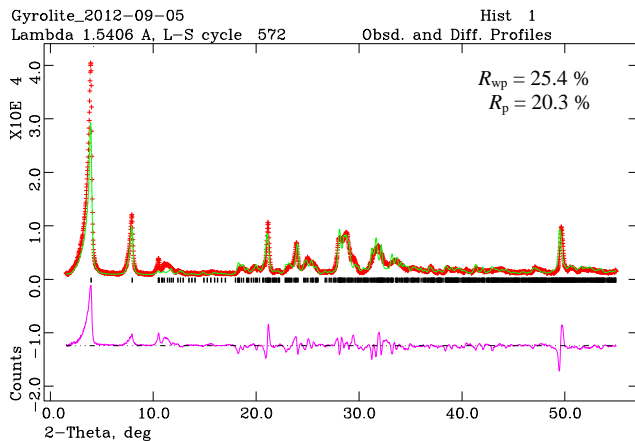

Fig. 6. The initial Rietveld fitting plot of the observed (in red), calculated (in green) and difference (in pink) between the observed and calculated patterns of gyrolite
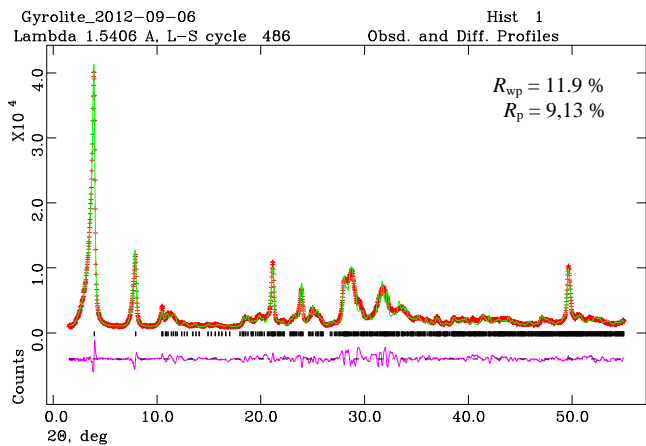

Fig. 7. The Rietveld fitting plot of the observed (in red), refined (in green) and difference (in pink) between the observed and refined patterns of gyrolite after the completion of Rietveld refinement using restraints on bond lengths

Table 2. Atomic coordinates, fractional occupancy and temperature displacement parameters for the interlayer sheet X of synthetic gyrolite after the initial Rietveld refinement

Atom	x	y	z	Occupancy	U_{iso}, Å^2
Ca4	0.341	0.697	0.4963	1	0.024
O1	0.294	0.884	0.5452	1	−0.011
O2	0.079	0.542	0.4372	1	−0.011
O3	0.396	0.480	0.4537	1	−0.011
O4	0.591	0.842	0.5500	1	−0.011
O5	0.765	0.772	0.4423	1.014	−0.011
O6	0.952	0.845	0.5846	1.014	−0.011
O7	0.863	0.123	0.5478	1.014	−0.011
Ca5	0	0	0.5	0.020	0.024

Unit cell parameters of synthetic gyrolite after this stage of the refinement have obtained following values: $a = 0.9737(3)$ nm, $b = 0.9729(3)$ nm, $c = 2.2482(5)$ nm, $\alpha = 95.44(3)°$, $\beta = 91.49(3)°$, $\gamma = 120.08(1)°$.

Refinement of the individual occupancy parameters of interlayer sheet atoms yields nearly zero value of Ca5 atom, as seen in last row in Table 2. This means that Ca5 atom was removed from the special position of the interlayer sheet (Fig. 8).
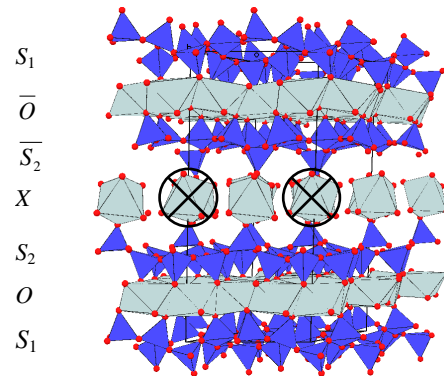

Fig. 8. The crystal structure of synthetic pure gyrolite after the initial Rietveld refinement. Ca5 atom was removed from special position of the unit cell (crosses show no existence of Ca octahedral)

A possible atomic arrangement in site of former Ca5 octahedral was solved using the Monte-Carlo based global optimization with parallel tempering algorithm, as implemented in the FOX program (Fig. 9). The structure of the interlayer sheet was rearranged by the introduction of three unique H_2O molecules having random positions and orientations with an average O-H bond length of 0.095 nm.
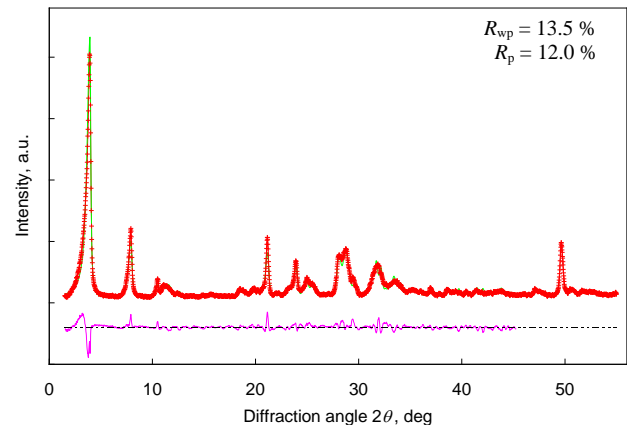

Fig. 9. The X-ray diffraction plot of the observed (in red), calculated (in green) and difference (in pink) between the observed and calculated patterns after the global optimization of crystal structure of gyrolite using program FOX

Atomic positions and fractional occupation parameters obtained after global optimization are presented in the last nine rows of Table 3. Atoms O7, H5 and H6 after global optimization have obtained negative occupancy that has no physical sense. It means that one H_2O molecule should to be removed.

This result agrees well with the values obtained during further Rietveld refinement using the same crystal structure model of gyrolite in which one Ca5 atom was replaced by three H_2O molecules and starting atomic coordinates were included from Table 3. The resultant plot fit is shown in Figure 10 and atomic arrangement in Table 4.

Table 3. Atomic coordinates, fractional occupancy, and thermal parameters for the interlayer sheet *X* after the simulation of gyrolite crystal structure parameters by global optimization algorithm using program FOX

| Atom	x	y	z	Occupancy	U_{iso}, Å^2
Ca4	0.3205	0.6868	0.4966	1	0.0013
O1	0.2971	0.8853	0.5436	1	0.0013
O2	0.0773	0.5409	0.4383	1	0.0013
O3	0.3963	0.4801	0.4547	1	0.0013
O4	0.5889	0.8443	0.5518	1	0.0013
O5	0.7449	0.8716	0.4437	1.606	0.0013
O6	0.2224	0.4597	0.5972	1.502	0.0013
O7	0.4453	0.5799	0.5677	−1.038	0.0013
H1	0.7232	0.9558	0.4325	1.601	0.0013
H2	0.8619	0.9235	0.4481	1.601	0.0013
H3	0.1224	0.3739	0.5739	1.502	0.0013
H4	0.3036	0.4410	0.5801	1.502	0.0013
H5	0.5114	0.6694	0.5437	−1.038	0.0013
H6	0.3672	0.4936	0.5316	−1.038	0.0013
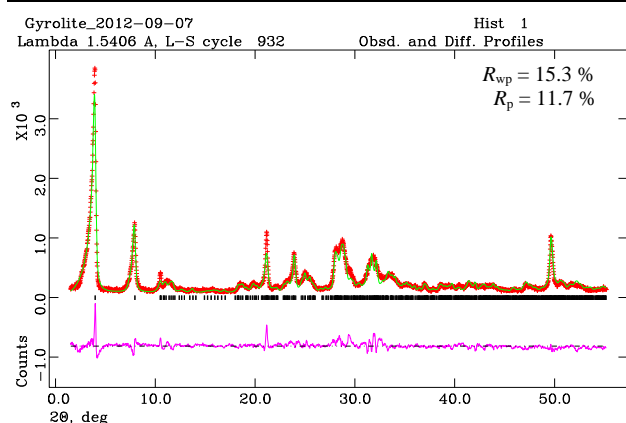
Fig. 10. The Rietveld fitting plot of the observed (in red), calculated (in green) and difference (in pink) between the observed and calculated patterns of gyrolite after refinement of gyrolite crystal structure

Table 4. Atomic coordinates, fractional occupancy, and thermal parameters for the interlayer sheet *X* of gyrolite after the Rietveld refinement

Atom	x	y	z	Occupancy	U_{iso}, Å^2
Ca4	0.3400	0.6880	0.4980	1	0.00038
O1	0.2920	0.8810	0.5451	1	0.00063
O2	0.0802	0.5410	0.4376	1	0.00063
O3	0.3900	0.4790	0.4548	1	0.00063
O4	0.5920	0.8442	0.5500	1	0.00063
O5	0.7637	0.7710	0.4413	0.91	0.00063
O6	0.9501	0.8456	0.5849	0.99	0.00063
O7	0.8634	0.1253	0.5475	−0.05	0.00063
H1	0.7820	0.6860	0.4210	0.91	0.01266
H2	0.8567	0.8360	0.4680	0.91	0.01266
H3	0.9722	0.8050	0.5472	0.99	0.01266
H4	0.8680	0.8680	0.5737	0.99	0.01266
H5	0.7559	0.0470	0.5323	−0.05	0.01266
H6	0.8510	0.1910	0.5790	−0.05	0.01266

When the current stage of the Rietveld structure refinement was finished the same atoms O7, H5 and H6

were removed from the unit cell of gyrolite interlayer sheet as it happened too in the global optimization (Table 4). The refined values listed in Table 4 have been used as initial structure parameters for the final crystal structure refinement of synthetic pure gyrolite. During the refinement the most possible atomic arrangement in the interlayer sheet *X* of unit cell of gyrolite was achieved. The final quality of the refinement was quantified by the obtained following figures of merit: weighted profile residual $R_{wp} = 11.4$ % and profile residual $R_p = 8.57$ % for a total refined 200 variables. The satisfactory convergence was achieved and the final fit is illustrated in Figure 11.

Unit cell parameters of synthetic pure gyrolite after final stage of the refinement have obtained following values: $a = 0.9713(2)$ nm, $b = 0.9715(2)$ nm, $c = 2.2442(3)$ nm, $\alpha = 95.48(2)$º, $\beta = 91.45(2)°$, $\gamma = 120.05(3)°$.
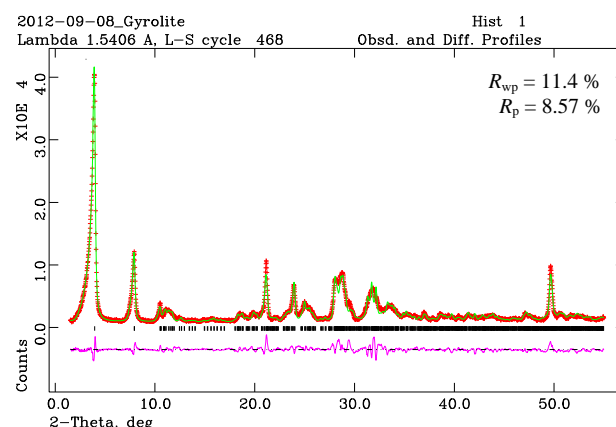

Fig. 11. The final Rietveld refinement of pure gyrolite crystal structure using restraints on bond lengths and two molecules of H$_2$O instead of Ca cation in the interlayer sheet of the unit cell of gyrolite. The observed (in red), calculated (in green) and difference (in pink) between the observed and calculated X-ray diffraction patterns

The resultant values of refined structural parameters are listed in Table 5.

Table 5. Atomic coordinates, fractional occupancy, and thermal parameters for the interlayer sheet *X* of gyrolite after the final Rietveld refinement

Atom	x	y	z	Occupancy	U_{iso}, Å^2
Ca4	0.3291	0.6934	0.5000	1	0.00038
O1	0.3180	0.8940	0.5523	1	0.00063
O2	0.0756	0.5470	0.4424	1	0.00063
O3	0.4070	0.4970	0.4551	1	0.00063
O4	0.5790	0.8440	0.5575	1	0.00063
O5	1.0090	1.2250	0.4508	1	0.00063
O6	−0.074	0.0900	0.5513	1	0.00063
H1	1.0290	1.1910	0.4099	1	0.00127
H2	1.0200	1.3320	0.4480	1	0.00127
H3	−0.066	0.0090	0.5230	1	0.00127
H4	0.0380	0.1650	0.5690	1	0.00127

The complete geometrical characteristics of final crystal structure are presented in Figure 12. The final most likelihood arrangement of H$_2$O molecules in refined crystal structure of gyrolite are shown with arrow.
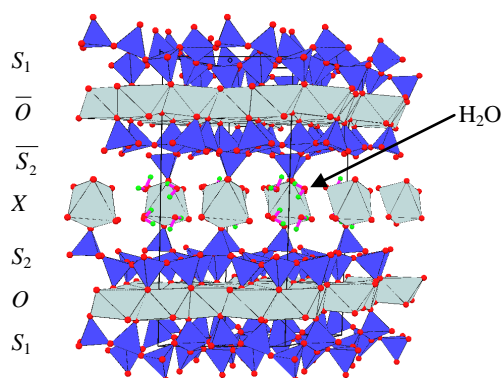
Fig. 12. The crystal structure of synthetic pure gyrolite as determined during the final Rietveld refinement

CONCLUSIONS

The crystal structure of synthetic pure gyrolite using X-ray diffraction, Le Bail, Rietveld and modeling methods was investigated and refined. The lattice parameters were calculated to be: $a = 0.9713(2)$ nm, $b = 0.9715(2)$ nm, $c = 2.2442(3)$ nm, $\alpha = 95.48(2)°$, $\beta = 91.45(2)°$, $\gamma = 120.05(3)°$. The Ca atom was not found in the special position (0, 0, 0.5) of pure gyrolite unit cell where Merlino S. in natural gyrolite identified Na atom. Instead of Ca atom two H_2O molecules in octahedral site of pure gyrolite unit cell were solved and refined by global optimization and Rietveld methods.

REFERENCES

1. **Miyake, M., Iwaya, M., Suzuki, T., Kakehi, H., Mitsuda,** T. Aluminum-Substituted Gyrolite as Cation Exchanger *Journal of the American Ceramic Society* 73 1990: pp. 3524−3527.
2. **El-Korashy, S. A.** Cation Exchange of Alkali Metal Hydroxides with Some Hydrothermally Synthesized Calcium Silicate Compounds *Journal of Ion Exchange* 15 2004: pp. 2−9.
3. **Tits, J., Wieland, E., Müller, C. J., Landesman, C., Bradbury, M. H.** A Wet Chemistry Study of the Strontium Binding by Calcium Silicate Hydrates *Journal of Colloid and Interface Science* 300 2006: pp. 78−87.
4. **Kasperaviciute, V., Baltakys, K., Siauciunas, R.** The Sorption Properties of Gyrolite for Copper Ions *Ceramics-Silikaty* 52 2008: pp. 95−101.
5. **Bankauskaite, A., Baltakys, K.** The Sorption of Copper Ions by Gyrolite in Alkaline Solution *Materials Science-Poland* 27 2009: pp: 899−908.
6. **Coleman, N. J.** Interactions of Cd(II) with Waste-derived 11 Å Tobermorites *Separation and Purification Technology* 48 2006: pp. 62−70.
   http://dx.doi.org/10.1016/j.seppur.2005.07.021
7. **Coleman, N. J., Brassington, D. S., Raza, A., Mendham, A. P.** Sorption of Co^{2+} and Sr^{2+} by Waste-derived 11 Å Tobermorite *Waste Management* 26 2006: pp. 260−267.
8. **Siauciunas, R., Janickis, V., Palubinskaite, D., Ivanauskas, R.** The Sorption Properties of Tobermorite Modified with Na^+ and Al^{3+} Ions *Ceramics-Silikaty* 4 2004: pp. 876−882.
9. **Winters, M. A., Richter, J. D., Sagar, S. L., Lee, A. L., Lander, R. J.** Plasmid DNA Purification by Selective Calcium Silicate of Closely Related Impurities *Biotechnology Progress* 19 2003: pp. 440−447.
10. **Baltušnikas, A., Lukošiūtė, I., Baltakys, K.** XRD Characterization of Organically Modified Gyrolite *Materials Science (Medžiagotyra)* 15 2009: pp. 325−328.
11. **Shaw, S., Henderson, C., Clark, S.** In-situ Synchrotron Study of the Kinetics, Thermodynamics, and Reaction Mechanisms of the Hydrothermal Crystallization of Gyrolite *American Mineralogist* 87 2002: pp. 533−541.
12. **Baltakys, K., Siauciunas, R.** Physically and Chemically Bound H_2O in the Gyrolite Structure *Materials Science - Poland* 27 2009: pp. 255−263.
13. **Baltakys, K., Siauciunas, R., Kitrys, S.** Surface Microstructure and Specific Surface Area of Pure and Na-substituted Gyrolite *Materials Science - Poland* 26 2008: pp. 633−645.
14. **Baltakys, K., Eisinas, A., Dizhbite, T., Jasina, L., Šiaučiūnas, R., Kitrys, S.** The Influence of Hydrothermal Synthesis Conditions on Gyrolite Texture and Specific Surface Area *Materials and Structures* 44 2011: pp. 1687−1701.
15. **Nocun-Wczelik, W.** Effect of Some Inorganic Admixtures on the Formation and Properties of Calcium Silicate Hydrates Produced in Hydrothermal Conditions *Cement and Concrete Research* 27 1997: pp. 83−92.
16. **Baltakys, K., Siauciunas, R.** Gyrolite Formation in CaO-SiO₂·nH₂O-γ-Al₂O₃-Na₂O-H₂O System under Hydrothermal Conditions *Polish Journal of Chemistry* 81 2007: pp. 103−114.
17. **Merlino, S.** Gyrolite: Its Crystal Structure and Crystal Chemistry *Mineralogical Magazine* 52 1988: pp. 377−387.
18. **Lachowski, E. E., Murray, L. W., Taylor, H. F. W.** Truscottite: Composition and Ionic Substitutions *Mineralogical Magazine* 43 1979: pp. 333−336.
   http://dx.doi.org/10.1180/minmag.1979.043.327.03
19. **Merlino, S.** The Structure of Reyerite, (Na,K)₂Ca₁₄Si₂₂A1₂O₅₈(OH)₈·6H₂O *Mineralogical Magazine* 52 1988: pp. 247−256.
   http://dx.doi.org/10.1180/minmag.1988.052.365.12
20. **Ferraris, G.** Tungusite: New Data, Relationship with Gyrolite and Structural Model *Mineralogical Magazine* 59 1995: pp. 535−543.
   http://dx.doi.org/10.1180/minmag.1995.059.396.13
21. **Renaudin, G., Russias, J., Leroux, F., Frizon, F., Caudit-Coumes, C.** Structural Characterization of CSH and CASH Samples − Part I: Long-range Order Investigated by Rietveld Analyses *Journal of Solid State Chemistry* 182 2009: pp. 3312−3319.
22. **Stumm, A., Garbev, K., Beuchle, G., Blacka, L., Stemmermann, P., Nüesch, R**. Incorporation of Zinc into Calcium Silicate Hydrates. Part I: Formation of C–S–H(I) with C/S=2/3 and Its Isochemical Counterpart Gyrolite *Cement and Concrete Research* 35 2005: pp. 1665−1675.
23. **Baltušnikas, A., Lukošiūtė, I, Levinskas, R., Grybėnas, A., Baltakys, K., Eisinas, A.** Analysis of Rietveld Method Application for Gyrolite Crystal Structure Refinement *Materials Science (Medžiagotyra)* 18 (4) 2012: pp. 379−384.
24. **Le Bail, A., Duroy, H., Fourquet, J. L.** Ab-initio Structure Determination of LiSbWO6 by X-ray Powder Diffraction *Materials Research Bulletin* 23 (3) 1988: pp. 447−452.
25. **Larson, A. C., Von Dreele, R. B.** General Structure Analysis System (GSAS) Los Alamos National Laboratory Report LAUR. 1994: pp. 86−748.
26. **Toby, B. H.** EXPGUI, a Graphical User Interface for GSAS *Journal of Applied Crystallography* 34 2001: pp. 210−213.
   http://dx.doi.org/10.1107/S0021889801002242
27. **Finger, L., Kroeker, M. Toby, B.** DRAWxtl V5.3. A Program to Make Ball-and-stick, or Polyhedral Crystal Structure. 2007.
   http://www.lwfinger.com/drawxtl/dxtlman.html
28. **Favre-Nicolin, V., Cerny, R.** FOX, 'Free Objects for Crystallography': A Modular Approach to ab initio Structure Determination from Powder Diffraction *Journal of Applied Crystallography* 35 2002: pp. 734−743.
29. PDF-2 International Centre for Diffraction Data. 12 Campus Boulevard Newtown Square, PA 19073−3273 USA.